Modulation response of nanoLEDs and nanolasers exploiting Purcell enhanced spontaneous emission

Skovgård, Troels Suhr; Gregersen, Niels; Yvind, Kresten; Mørk, Jesper

Published in:
Optics Express

Link to article, DOI:
10.1364/OE.18.011230

Publication date:
2010

Document Version
Publisher's PDF, also known as Version of record

Modulation response of nanoLEDs and nanolasers exploiting Purcell enhanced spontaneous emission

T. Suhr[1,*], N. Gregersen[1], K. Yvind[1], and J. Mørk[1]

[1]*DTU Fotonik, Department of Photonics Engineering, Technical University of Denmark. DTU Fotonik, Ørsteds Plads 343, DK2800 Kgs. Lyngby Denmark*
**suhr@fotonik.dtu.dk*

The modulation bandwidth of quantum well nanoLED and nanolaser devices is calculated from the laser rate equations using a detailed model for the Purcell enhanced spontaneous emission. It is found that the Purcell enhancement saturates when the cavity quality-factor is increased, which limits the maximum achievable spontaneous recombination rate. The modulation bandwidth is thereby limited to a few tens of GHz for realistic devices.

OCIS codes: (060.4080) Modulation; (140.3948) Microcavity devices; (230.3670) Light-emitting diodes; (140.5960) Semiconductor lasers; (320.7090) Ultrafast lasers.

References and links

1. Y. Akahane, T. Asano, B.-S. Song, and S. Noda, "High-Q photonic nanocavity in a two-dimensional photonic crystal," Letters to Nature **425**(6961), 944–947 (2003).
2. E. M. Purcell, "Spontaneous emission probabilities at radio frequencies," Phys. Rev. **69**, 681 (1946).
3. Y. Yamamoto, S. Machida, and G. Björk, "Microcavity semiconductor laser with enhanced spontaneous emission," Phys. Rev. A **44**(1), 657–668 (1991).
4. O. Painter, R. K. Lee, A. Scherer, A. Yariv, J. D. O'Brien, P. D. Dapkus, and I. Kim I, "Two-dimensional photonic band-Gap defect mode laser," Science **284**(5421), 1819–1821 (1999).
5. H. Altug, D. Englund, and J. Vučković, "Ultrafast photonic crystal nanocavity laser," Nat. Phys. **2**(7), 484–488 (2006).
6. E. K. Lau, A. Lakhani, R. S. Tucker, and M. C. Wu, "Enhanced modulation bandwidth of nanocavity light emitting devices," Opt. Express **17**(10), 7790–7799 (2009).
7. L. A. Coldren, and S. W. Corzine, *Diode Lasers and Photonic Integrated Circuits* (John Wiley & Sons, inc., New York, 1995).
8. J. D. Jackson, *Classical Electrodynamics* (John Wiley & Sons, inc., New York, 1998)
9. A. Mecozzi, and J. Mørk, "Saturation induced by picosecond pulses in semiconductor optical amplifiers," J. Opt. Soc. Am. B **14**(4), 761–770 (1997).
10. J. D. Joannopoulos, S. G. Johnson, and J. N. Winn, *Photonic Crystals: Molding the Flow of Light* (Princeton University Press, New Jersey, 2008).
11. J.-M. Gerard, "Solid-state cavity-quantum electrodynamics with self-assembled quantum dots", in *Single Quantum Dots, Fundamentals, Applications and New Concepts*, P. Michler (Springer, Berlin, 2003), pp. 269–314.
12. H. Yokoyama, and S. D. Brorson, "Rate equation analysis of microcavity lasers," J. Appl. Phys. **66**(10), 4801 (1989).
13. T. Baba, "Photonic crystals and microdisk cavities based on GaInAsP-InP system," IEEE J. Sel. Top. Quantum Electron. **3**(3), 808 (1997).
14. D. Englund, D. Fattal, E. Waks, G. Solomon, B. Zhang, T. Nakaoka, Y. Arakawa, Y. Yamamoto, and J. Vucković, "Controlling the spontaneous emission rate of single quantum dots in a two-dimensional photonic crystal," Phys. Rev. Lett. **95**(1), 013904 (2005).
15. S. M. Barnett, and R. Loudon, "Sum rule for modified spontaneous emission rates," Phys. Rev. Lett. **77**(12), 2444–2446 (1996).
16. T. Baba, D. Sano, K. Nozaki, K. Inoshita, Y. Kuroki, and F. Koyama, "Observation of fast spontaneous emission decay in GaInAsP photonic crystal point defect nanocavity at room temperature," Appl. Phys. Lett. **85**(18), 3989–3991 (2004).
17. M. P. Marder, *Condensed Matter Physics* (John Wiley & Sons, inc., New York, 2000).
18. R. S. Tucker, "High-speed modulation of semiconductor lasers," J. Lightwave Technol. **3**(6), 1180–1192 (1985).

#126340 - $15.00 USD Received 31 Mar 2010; revised 6 May 2010; accepted 9 May 2010; published 12 May 2010

Introduction

In the emerging field of photonic signal processing there is an expressed need for small and efficient light emitters that can be integrated in photonic circuits and which have large modulation bandwidths. Today's fastest diode lasers exhibit modulation speeds on the order of a few tens of GHz and nanolasers and nanoLEDs have been suggested as interesting alternatives. In the past two decades process technology has matured sufficiently to enable fabrication of active cavities with high quality-factors and low mode volumes [1], where the Purcell enhancement of spontaneous emission [2] can become large enough to affect the dynamics of the device [3–6]. Early predictions of the properties of nanolasers by Altug *et al.* [5], based on an analysis of the laser rate equations with a phenomenological Purcell enhancement of the spontaneous emission rate, suggested modulation speeds exceeding 100 GHz. Recently, the same system was investigated numerically in a paper by Lau *et al.* [6] where the importance of gain suppression was pointed out and it was indicated that the ultrahigh modulation speeds reported by Altug *et al.* were the result of the measurement method and are in reality only achievable in non-lasing devices with ultralow mode volume. Because of the potentially very high Purcell factor, the dynamics of the device is very dependent on the details of the spontaneous emission and a rigorous treatment of spontaneous emission is needed. In this paper we therefore calculate the spontaneous emission from fundamental principles and study the effect on the dynamic properties of nanoLEDs and nanolasers. We find that the high-speed properties predicted in ref [6]. for nanoLEDs are deteriorated due to a reduction and saturation of the Purcell enhancement factor, which is intrinsic to quantum well and bulk active materials.

First, we will state the basic laser rate equations and a general expression for the 3dB-bandwidth. Then we will outline the model for the Purcell enhanced spontaneous emission rate and discuss the general behavior of the calculated rates. Next, the steady-state carrier and photon densities, the spontaneous and stimulated emission rates and the 3dB-bandwidth are calculated for two characteristic devices: one in the LED regime and one in the lasing regime and the results are discussed in the context of previous models. Finally, the 3dB-bandwidth is calculated for a wide range of nanoLEDs and nanolasers.

General rate equations and modulation response

Conventional diode lasers are well described in terms of the carrier (N) and photon (S) densities in the laser rate equations [6,7]

$$\dot{N} = J - R_c - R_b - R_{st} - R_{nr} \tag{1}$$

$$\dot{S} = \Gamma\left(R_c + R_{st}\right) - \frac{N}{\tau_p} \tag{2}$$

where J is the carrier injection into the active volume, Γ is the confinement factor and $\tau_p = Q/\omega_0$ is the lifetime of the photon in the cavity given by the quality (Q) factor and the cavity resonance frequency [8] (see Table 1 for parameter values used in this paper). The total carrier recombination rate has been separated into contributions from stimulated emission (R_{st}), spontaneous emission into the cavity (R_c), spontaneous emission into all other modes (R_b) and non-radiative losses (R_{nr}). For the latter we approximate $R_{nr} = N/\tau_{nr}$ with τ_{nr} being the non-radiative life time. For the stimulated emission we use

$$R_{st} = GS = \frac{v_g G_0}{1+\varepsilon S}\ln\left(\frac{N+N_s}{N_{tr}+N_s}\right)S \tag{3}$$

which is suitable for the quantum well type devices considered [7]. Here $v_g = c/n$ is the group velocity, G_0 is the material gain, N_{tr} is the transparency carrier density and N_s is a gain

#126340 - $15.00 USD Received 31 Mar 2010; revised 6 May 2010; accepted 9 May 2010; published 12 May 2010

parameter [7]. The gain, G, in Eq. (3) is inversely proportional to $1 + \varepsilon S$ [9] to include gain suppression due to spectral hole burning and carrier heating at high photon densities.

An important measure for the performance of laser diodes is the modulation bandwidth which can be estimated from a small-signal analysis of Eq. (1) and (2). Following a standard derivation (ref [7]. p. 195-201) the general form of the small-signal response function can be written as

$$H(\omega) = \frac{\omega_R^2}{\omega_R^2 - \omega^2 + i\omega\gamma_R} \tag{4}$$

Table 1. Definition and standard values of the parameters used in this paper. If nothing else is specified in the text, the value stated here has been used in the calculations.

Parameter	Description	Value
Γ	Confinement factor	0.1 [6]
n	Refractive index	3.5 [7]
G_0	Material gain parameter	1.284×10^5 m^{-1} [6]
N_{tr}	Transparency density	1.2×10^{24} m^{-3} [6]
N_s	Logarithmic gain parameter	0.92 N_{tr} [6]
ε	Gain suppression factor	18 N_{tr}^{-1} [6]
τ_{sp}	Spontaneous recombination time	1 ns [6]
τ_{nr}	Non-radiative recombination time	1 ns [6]
τ_{21}	Differential recombination time	125 ps
$h\nu_0$	Cavity resonance	0.8 eV [7]
$h\nu_L$	Lower photonic band edge	0.9 $h\nu_0$ [10]
$h\nu_U$	Upper photonic band edge	1.1 $h\nu_0$ [10]
W	Quantum well width	8 nm [7]
m_e*	Effective electron mass	0.045 m_e [7]
m_h*	Effective hole mass	0.37 m_e [7]

where ω_R is the resonance frequency of the response function and γ_R is the damping. Both ω_R and γ_R will be defined below. Solving $|H(\omega_{3dB})|^2 = |H(0)|^2/2$ for the frequency gives the 3dB-bandwidth

$$f_{3dB} = \frac{1}{2\pi}\sqrt{\omega_R^2 - \frac{\gamma_R^2}{2} + \sqrt{\left(\omega_R^2 - \frac{\gamma_R^2}{2}\right)^2 + \omega_R^4}} \tag{5}$$

The terms R_c and R_b are spontaneous emission processes that depend only on the carrier density and not on the photon density, therefore, with Eq. (1) and (2), ω_R and γ_R are given by

$$\omega_R^2 = \frac{1}{\tau_p}\left(aS_0 + R_{c,N}\right) + \Gamma\left(\frac{1}{\tau_{nr}} + R_{b,N}\right)\left(a_p S_0 + \frac{R_c}{S_0}\right) \tag{6}$$

and

$$\gamma_R = \frac{1}{\tau_{nr}} + R_{c,N} + R_{b,N} + S_0\left(a + \Gamma a_p\right) + \frac{\Gamma R_c}{S_0} \tag{7}$$

where N_0 and S_0 are steady-state carrier and photon densities and $a = dG/dN$, $a_p = -dG/dS$, $R_{c,N} = dR_c/dN$ and $R_{b,N} = dR_b/dN$. In the following we specify R_c and R_b and use Eq. (5) - (7) to calculate the modulation response.

#126340 - $15.00 USD Received 31 Mar 2010; revised 6 May 2010; accepted 9 May 2010; published 12 May 2010

Purcell enhanced spontaneous emission

For nanocavity devices with high Q and low mode volume (V) the Purcell effect should be taken into account when calculating the spontaneous emission [2,5,6,11]. The Purcell factor reflects the increased spectral density of a single mode centered in a cavity and can be written as

$$F = \frac{6}{\pi^2}\frac{Q}{V_n} \tag{8}$$

where $V_n = V/(\lambda/(2n))^3$ is the mode volume in half wavelengths. There exist a number of different definitions of the Purcell effect, but here we take F to be the spontaneous emission rate into the cavity mode relative to the spontaneous emission rate in a bulk (homogeneous) medium at the same spectral position and use Eq. (8) to describe its magnitude. We consider two models for spontaneous emission, which include the Purcell enhancement.

Linear Model

In conventional semiconductor diodes operated near threshold the spontaneous emission can be approximated as being linear in the carrier density, $R_{sp} = N/\tau_{sp}$, where τ_{sp} is the spontaneous lifetime in bulk. In the linear model the spontaneous emission is often split so that $R_c = \beta R_{sp}$ and $R_b = (1-\beta)R_{sp}$, where $\beta = R_c/R_{sp}$ is the spontaneous emission factor.

The Purcell effect is taken into account phenomenologically by multiplying F onto R_c [5,6,12,13] to include the relatively larger emission into the cavity. We use the spontaneous emission terms from ref [6]. as an example of the linear model, i.e.

$$R_c = \beta F \frac{N}{\tau_{sp}} \tag{9}$$

$$R_b = (1-\beta)\frac{N}{\tau_{sp}} \tag{10}$$

Inserting Eq. (9) and (10) into Eq. (6) and (7) above, we thus recover Eq. (9) and (10) of ref [6]. For systems with $\beta \sim 1$ this model assumes that the Purcell effect acts on all the carriers in the system as it does not take into account the details in the optical density-of-states (DOS), which are important when discussing devices with large Purcell factors. Furthermore, the linear model is only valid close to its Taylor expansion point.

Full Model

In the full model we follow ref [7]. and write the differential spontaneous recombination rate for a semiconductor device in terms of the differential carrier population, dN_2, as $dR_{sp} = A_{21}dN_2$, where the Einstein coefficient (A_{21}) is proportional to the optical DOS (ρ_{op}) and the B_{21} coefficient, i.e. $A_{21} = h\nu\rho_{op}B_{21}$. dN_2 can be written in terms of the electron (f_2) and hole (f_1) Fermi functions and the reduced electronic DOS (ρ_{el}) as $dN_2 = \rho_{el}f_2(1-f_1)dE_{21}$ and homogeneous broadening is taken into account by convoluting with the lineshape function $L(E - h\nu)$, which is usually taken to be a Lorentzian. Integrating over energy we arrive at an expression for spontaneous emission rate (ref [7]. p. 459-472)

$$R_{sp} = \iint \rho_{el}(E) f_2(E)\left(1 - f_1(E)\right) A_{21}(h\nu) L(E - h\nu)\,\mathrm{d}h\nu\,\mathrm{d}E \tag{11}$$

The optical DOS is modeled as the bulk DOS plus a Lorentzian shaped cavity spectrum [14] placed in the center of a photonic bandgap, i.e.

$$\rho_{op} = \frac{8\pi\nu^2}{v_g^3}\left(H(h\nu_L - h\nu) + H(h\nu - h\nu_U)\right) + \frac{F}{B_{21}h\nu\tau_{21}}\frac{\Gamma_p^2}{(h\nu - h\nu_0)^2 + \Gamma_p^2} \tag{12}$$

#126340 - $15.00 USD Received 31 Mar 2010; revised 6 May 2010; accepted 9 May 2010; published 12 May 2010

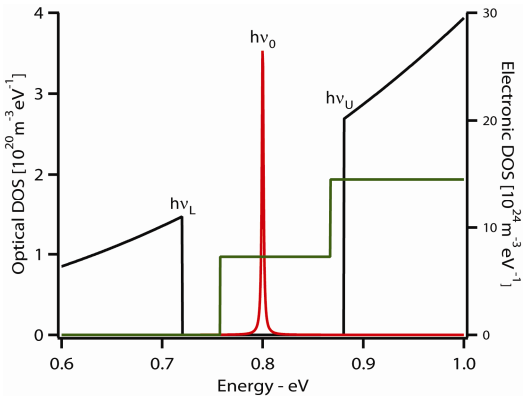

Fig. 1. The relative positions of the background optical DOS (black), the cavity optical DOS (red) and the electronic well DOS (green).

Here H is the Heaviside function and the cavity is centered at $h\nu_0 = (h\nu_U - h\nu_L)/2$, with $h\nu_L$ ($h\nu_U$) being the lower (upper) edge of the photonic band gap and $\Gamma_p = 2\hbar/\tau_p$ the width of the Lorentzian (c.f. Figure 1). The Einstein B_{21} coefficient is found by setting $A_{21}(h\nu_0) = 1/\tau_{21} = h\nu_0 B_{21}\rho_{op}(h\nu_0)$, where the differential recombination time (τ_{21}) is chosen so that the bulk spontaneous emission time (τ_{sp}) is recovered in the absence of the cavity, i.e. so that $R_{sp}(N_{tr}) = N_{tr}/\tau_{sp}$ in bulk. We then have

$$A_{21}(h\nu) = \frac{1}{\tau_{21}}\left[\left(\frac{h\nu}{h\nu_0}\right)^3 \left(H(h\nu_L - h\nu) + H(h\nu - h\nu_U)\right) + \frac{F\Gamma_p^2}{(h\nu - h\nu_0)^2 + \Gamma_p^2}\right] \quad (13)$$

This model for the optical DOS thus describes the Purcell enhancement as the redistribution of the modes, which are suppressed by the photonic bandgap, into the cavity. The increase in the DOS near the edges of the photonic bandgap, which is usually observed in photonic crystals [17] and follows a sum rule [15], is not taken into account.

The reduced electronic DOS is given by [7]

$$\rho_{el}(E) = \frac{m_r}{\pi\hbar^2 W}\sum_{n=1}^{\infty} H\left(E - \left(E_g + n^2 E_1\right)\right) \quad (14)$$

where $m_r = (m_e^* m_h^*)/(m_e^* + m_h^*)$ is the reduced effective mass, m_e^* (m_h^*) is the effective electron (hole) mass, W is the well width, E_g is the bandgap energy and $E_1 = h^2/(8m_r W^2)$ is the energy of the first energy level in a quantum well with infinitely high barriers. The use of a more accurate description of the quantum well does not change the conclusions of the paper.

In this model (Eq. (11) - (14)), which we will refer to as the "full model", R_b is the integral over the bulk part of Eq. (13) while the Lorentzian part gives R_c. Although the full model specifically describes quantum well devices it is also suitable for bulk devices if an appropriate electronic DOS is chosen. Quantum dot devices, however, are governed by a different set of laser rate equations than Eq. (1) and (2) and should account for the dynamics in both the wetting layer and quantum dot levels. Furthermore, the electronic DOS for quantum dots is markedly different from that of bulk and quantum wells and including quantum dots in the treatment would make the discussion less clear. Although the use of quantum dot structures may be very promising, we therefore only treat quantum well (and bulk) devices in this paper.

#126340 - $15.00 USD Received 31 Mar 2010; revised 6 May 2010; accepted 9 May 2010; published 12 May 2010

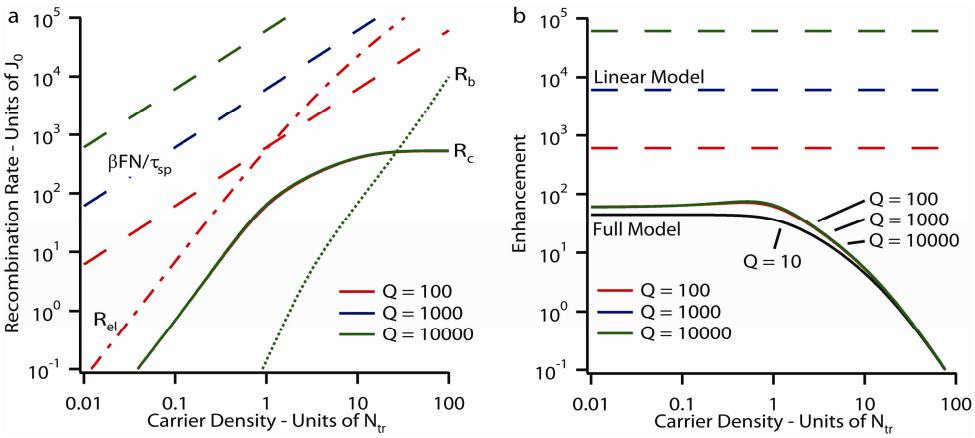

Fig. 2. a) The calculated spontaneous recombination rates for Q equal to 100 (red), 1000 (blue) and 10000 (green). In the full model the emission into the cavity (solid lines) is several orders of magnitude lower than in the linear model (dashed lines). Also shown is the emission into the background in the full model (dotted line) and R_{el} for Q = 100 (dot-dashed line). β is 0.94 and V_n is 0.1. b) The effective Purcell factor in the full model (solid lines) and in the linear model (dashed lines) for Q equal to 100 (red), 1000 (blue) and 10000 (green). The effective Purcell factor for Q = 10 is also shown.

Saturation of Purcell enhancement

In Fig. 2a the spontaneous emission calculated in the linear and the full model are compared. It is seen that the spontaneous emission in the full model is significantly lower than in the linear model and does not have a linear dependence on N. To see clearly the contribution from the electronic part of Eq. (11) we also plot (for a Q of 100)

$$R_{el} = \iint \rho_{el}(E) f_2(E)\left(1 - f_1(E)\right)\frac{F}{\tau_{21}} L(E - h\nu)\,\mathrm{d}h\nu\,\mathrm{d}E$$
$$\approx \frac{F}{\tau_{21}} \int \rho_{el}(E) f_2(E)\left(1 - f_1(E)\right)\mathrm{d}E \qquad (15)$$

As can be seen from Fig. 2a, R_{el} approaches the slope of the linear model for high carrier density, i.e. for the quasi-Fermi level separation high above the electronic band edge, where the integral in Eq. (15) is almost equal to the carrier density. For low carrier density R_{el} follows R_c, although R_c is somewhat smaller due to the limiting effect of the cavity DOS. The saturation of R_c for $N > N_{tr}$ is not seen in R_{el} and originates from the finite quantum well DOS and associated band filling effects at the cavity resonance E_0, i.e. the quasi-Fermi level separation becomes much larger than E_0 so that $f_2\,(1 - f_1) \sim 1$ near E_0.

Perhaps the most interesting feature in Fig. 2a is that R_c does not increase with the Q-factor in the full model. This can be explained by evaluating the integral over frequency in Eq. (11). This is usually done by assuming the homogeneous broadening term, $L\,(E - h\nu)$, to be sharply peaked at $h\nu = E$ compared to the other terms in Eq. (11) so that it can be replaced by a Dirac delta-function. However, for high-Q cavities the cavity linewidth can easily become smaller than the homogeneous broadening and in this case the integral over frequency in Eq. (11) should be evaluated exactly. The results in the present model, however, are not significantly changed when evaluating the frequency integral exactly using a Lorentzian for the homogeneous broadening as the electronic DOS is much wider than the homogeneous broadening. Therefore, we will use $L(E - h\nu) = \delta(E - h\nu)$ from here on.

The cavity part of the integral over frequency in Eq. (11) becomes

#126340 - $15.00 USD Received 31 Mar 2010; revised 6 May 2010; accepted 9 May 2010; published 12 May 2010

$$\int \frac{F}{\tau_{21}} \frac{\Gamma_p^2}{\left(h\nu - h\nu_0\right)^2 + \Gamma_p^2} \delta\left(E - h\nu\right) dh\nu = \frac{F}{\tau_{21}} \frac{\Gamma_p^2}{\left(E - E_0\right)^2 + \Gamma_p^2} \tag{16}$$

which is a new Lorentzian. Then the cavity part of Eq. (11) becomes

$$R_c = \frac{F}{\tau_{21}} \int \frac{\Gamma_p^2}{\left(E - E_0\right)^2 + \Gamma_p^2} \rho_{el}\left(E\right) f_2\left(E\right)\left(1 - f_1\left(E\right)\right) A\left(E\right) \mathrm{dE} \tag{17}$$

Taking now the Lorentzian to be sharply peaked compared to the remaining terms in Eq. (17), which is the case for high Q, the remaining integral is effectively over the Lorentzian and we end up with

$$R_c = \frac{F}{\tau_{21}} \Gamma_p \pi \rho_{el}\left(E_0\right) f_2\left(E_0\right)\left(1 - f_1\left(E_0\right)\right) = \frac{12\hbar\omega_0}{\pi\tau_{21} V_n} \rho_{el}\left(E_0\right) f_2\left(E_0\right)\left(1 - f_1\left(E_0\right)\right) \tag{18}$$

which is independent of the Q-factor. Put in another way; when increasing the Q-factor, the increase in spontaneous emission into the cavity due to the Purcell enhancement is exactly cancelled by the simultaneous decrease in the effective integration range. Thus for increasing Q-factor, the Purcell enhancement reaches a maximum value when the cavity linewidth becomes δ-like compared to the other terms in Eq. (17), i.e. for Q larger than a few hundreds. The reduction thus originates from the mismatch between cavity bandwidth and the effective inhomogeneous broadening expressed by the electronic DOS. This agrees with the qualitative discussion given in ref [16].

Notice that the expression in Eq. (18) is still inversely proportional to the mode volume, so that the rate can be enhanced by lowering V_n. Note also that we here neglect features in the electronic DOS such as the exciton peak near the band edge, which may challenge the requirement that the electronic DOS be slowly varying. Deviations of this type from the assumed smooth electronic DOS do not affect the conclusions, but rather increase the Q-factor at which the Purcell enhancement saturates. However, a rigorous treatment of the electronic DOS is beyond the scope of this work.

Finally, we note that the emission into the background (R_b) shown in Fig. 2a is negligible for $N < 10\ N_{tr}$. Reducing the size of the photonic bandgap increases R_b, but the change is insignificant compared to R_c.

Effective Purcell factor

In order to make the subsequent discussion more transparent we now introduce an effective Purcell factor, which we define as

$$F_{eff} \equiv \frac{R_c}{R_{bulk}} \tag{19}$$

where R_{bulk} is the total spontaneous emission in the absence of a cavity, i.e.

$$\begin{aligned} &\text{(linear model)} \quad R_{bulk} = \frac{N}{\tau_{sp}} \\ &\text{(full model)} \quad R_{bulk} = \frac{1}{\tau_{sp}} \iint \rho_{el}\left(E\right) f_2\left(E\right)\left(1 - f_1\left(E\right)\right)\left(\frac{h\nu}{h\nu_0}\right)^3 L\left(E - h\nu\right) \mathrm{dh}\nu\, \mathrm{dE} \end{aligned} \tag{20}$$

The effective Purcell factor encompasses a number of the interesting effects described above, namely: the reduction of the Purcell enhancement due to the limited cavity bandwidth as compared to the inhomogeneous broadening, the saturation effect that occurs when the quasi-

#126340 - $15.00 USD Received 31 Mar 2010; revised 6 May 2010; accepted 9 May 2010; published 12 May 2010

Fermi level separation is much larger than the cavity resonance frequency and the increase in the β-factor, which follows from the Purcell enhanced emission into the cavity.

Using the definition in Eq. (19) and the expression for R_c in Eq. (9) the effective Purcell factor reduces to $F_{eff} = \beta F$ in the linear model. In the full model the effective Purcell factor is a function of the optical and electronic DOS and thus depends on Q, V_n and N and is therefore markedly different from the F_{eff} in the linear model.

The effective Purcell factors in the two models are plotted in Fig. 2b for the devices in Fig. 2a. For $N < N_{tr}$ we have F_{eff} in the full model almost constant, but lower than F_{eff} in the linear model due to the reduction originating from the limited cavity bandwidth. The decrease for $N > N_{tr}$ in the full model is a combination of the bandfilling effect and R_b growing large.

Results

We now proceed to calculate the steady-state carrier and photon densities, the spontaneous and stimulated emission and the 3dB-bandwidth for two specific devices in the linear and full model. To ease comparison, the β-factor calculated from the full model is used in the linear model. Device A has a Q-factor of 10^4 and a mode volume of 10 V_n and device B has a Q-factor of 10^2 and a mode volume of 0.1 V_n. The results for device A are plotted in Fig. 3a-c, and for device B in Fig. 3d-f.

In Fig. 3a the carrier and photon densities are shown as a function of the pump (in units of $J_0 = N_{tr}/\tau_{sp}$). For $J < J_0$ the carrier density in the linear model is much lower than in the full model. This is an effect of the reduction of the effective Purcell factor for high Q-factors in the full model, which limits F_{eff} to ~1 for low carrier density, whereas F_{eff} ~610 in the linear model. The higher spontaneous emission rate in the linear model explains the lower carrier density.

The carrier density in the full model clamps for $J \sim J_0$, when lasing sets in, and remains constant until $J \sim 100\ J_0$, where it again begins to increase. This increase is due to the gain suppression that becomes a significant process for $S_0 \sim 1/\varepsilon \sim 0.05\ N_{tr}$ and must be compensated by an increase of the linear gain. The β-factor is close to unity for the entire pumping range, which explains why the photon densities for the two models are equal for $J > 10\ J_0$ even though the linear model is dominated by spontaneous emission, while the full model is dominated by stimulated emission.

Figure 3b compares the spontaneous and stimulated emission for the two models. In the full model the spontaneous emission increases strongly until the carrier density clamps, where after the stimulated emission becomes dominant. The spontaneous emission remains constant until $J \sim 100\ J_0$, where the carrier density begins to increase again due to the gain suppression effect discussed above. In the linear model the carrier density is much lower than in the full model, giving a lower stimulated emission. This pushes the threshold pump up to around $J \sim 1000\ J_0$.

Several features observed in Fig. 3a and b are also found in the 3dB-bandwidth in Fig. 3c. In the full model the 3dB-bandwidth is dominated by spontaneous emission until $J \sim J_0$, after which stimulated emission dominates until gain suppression becomes important around $J \sim 100\ J_0$. Over the entire pumping range the 3dB-bandwidth does not exceed 20 GHz. In the linear model the high 3dB-bandwidth for $J < 100\ J_0$ is due to the high spontaneous emission and the drop-off for $J > 100\ J_0$ is due to the damping rate (γ_R) increasing more rapidly than the resonance frequency (ω_R) as explained in ref [2].

#126340 - $15.00 USD Received 31 Mar 2010; revised 6 May 2010; accepted 9 May 2010; published 12 May 2010

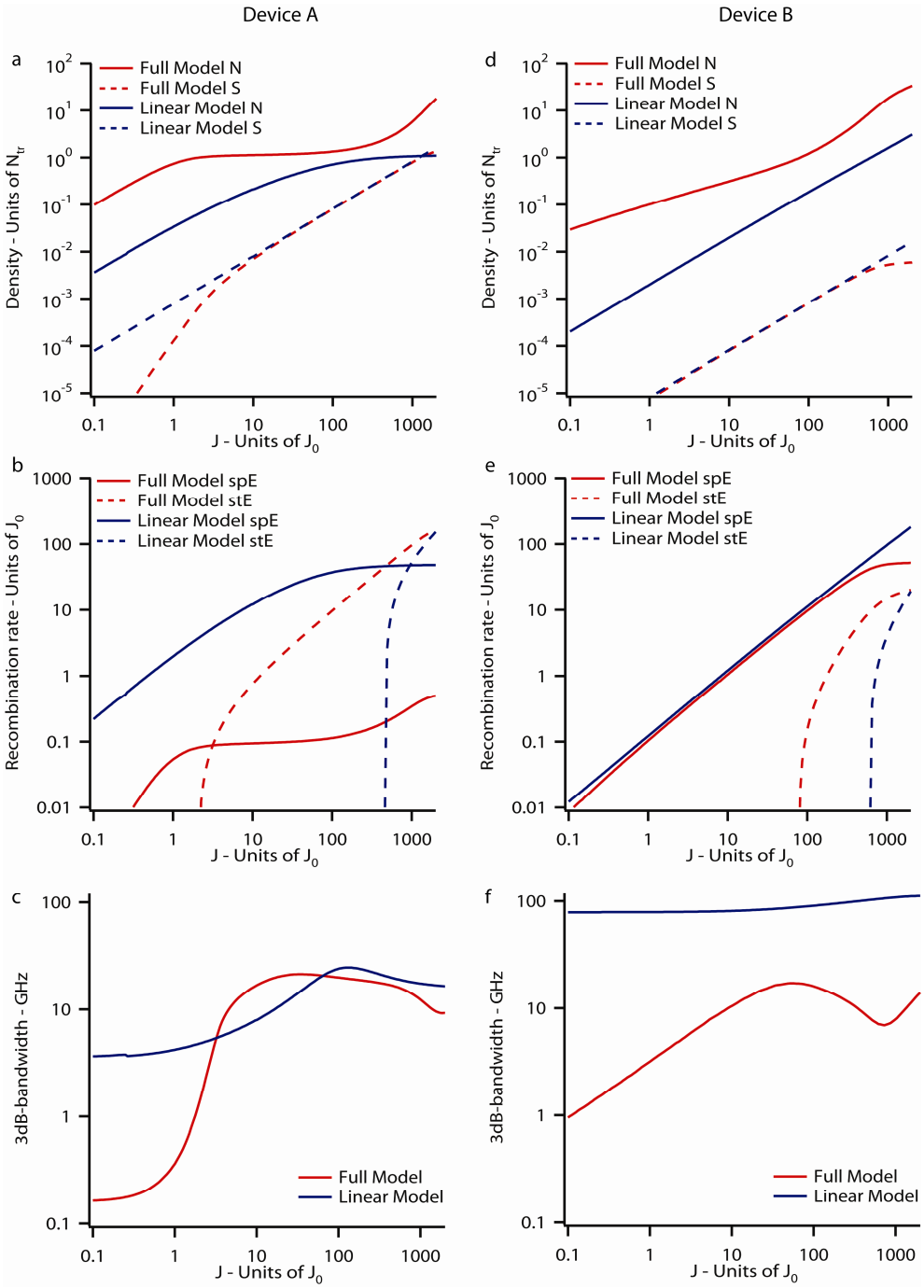

Fig. 3. Results from device A with $Q = 10^4$ and $V_n = 10$ and device B with $Q = 10^2$ and $V_n = 0.1$ plotted against pump (in units of $J_0 = N_{tr}/\tau_{sp}$). a) The carrier (solid) and photon (dashed) densities for device A, b) the spontaneous (solid) and stimulated (dashed) emission for device A and c) the 3dB-bandwidth for device A. d-f) are the same as a-c) but for device B. Both the full model (red) and the linear model (blue) are shown.

The results for device B are shown in Fig. 3d-f, where both the Q-factor and mode volume, V_n, are 100 times lower than in device A, so that F_{eff} remains ~610 in the linear

#126340 - $15.00 USD Received 31 Mar 2010; revised 6 May 2010; accepted 9 May 2010; published 12 May 2010

model, but changes to ~70 in the full model (for low carrier density). For this device the photon loss is 100 times larger than for device A and therefore the photon densities for the two models in Fig. 3d are 100 times lower. In the linear model, the relatively lower photon density is reflected in the carrier density, which is also lowered to balance the photon loss.

In the full model the carrier density is only slightly lower than for device A for $J < J_0$. This is because the spontaneous emission rate in the full model follows another dependence on N (approximately N^2) than in the linear model and therefore a smaller adjustment of N is necessary to compensate the lower photon density.

In Fig. 3e the spontaneous emission rate in the linear model is lower by a factor corresponding to the lowering of carrier density compared with device A. In the full model the spontaneous emission almost follows the increase in F_{eff}, but is also modified by the lower carrier density. In neither models the gain becomes large enough to initiate lasing and this is reflected in the carrier densities, which do not clamp in this device.

Figure 3f shows that the 3dB-bandwidth calculated in the two models differs significantly. The 3dB-bandwidth is almost an order of magnitude lower in the full model compared to the linear model. This can be explained by studying Eq. (5) in the LED regime, i.e. for dominating spontaneous emission. For the linear model Eq. (5) reduces to

$$f_{3dB} \approx \frac{1}{2\pi} \frac{1}{\sqrt{\tau_p^2 + \tau_{eff}^2}} \tag{21}$$

with the effective carrier life time

$$\frac{1}{\tau_{eff}} = \frac{F_{eff}}{\tau_{sp}} + \frac{1-\beta}{\tau_{sp}} + \frac{1}{\tau_{nr}} \approx \frac{F_{eff}}{\tau_{sp}} \tag{22}$$

Thus the high bandwidth observed in Fig. 3f is due to the effective Purcell factor growing large. In the full model the 3dB-bandwidth is also given by Eq. (21), but in this model we have

$$\frac{1}{\tau_{eff}} = F_{eff} \frac{dR_{bulk}}{dN} + \frac{dF_{eff}}{dN} R_{bulk} + \frac{dR_b}{dN} + \frac{1}{\tau_{nr}} \tag{23}$$

From Eq. (21), Eq. (23) and Fig. 2b the behavior of the 3dB-bandwidth in the full model now becomes clear.

For $J < 50\ J_0$ the effective Purcell factor is almost constant and $R_{b,N} \approx 0$, so that the first term in Eq. (23) determines τ_{eff}. For $50\ J_0 < J < 800\ J_0$ the term $R_{b,N}$ is still low, while F_{eff} starts to decrease so that the first term of Eq. (23) becomes smaller and the second term becomes negative, leading to a decrease in the 3dB-bandwidth. For $J > 800\ J_0$ the background emission increases sharply, making τ_{eff} decrease and leading to the final increase in the 3dB-bandwidth. Thus the 3dB-bandwidth in the full model is roughly an order of magnitude lower than in the linear model and this clearly underlines the necessity for a detailed description of the spontaneous emission.

The same analysis can be made for Fig. 3c for $J < 2J_0$, as spontaneous emission is also dominant in this pumping range. Here the effective Purcell factor in the full model is 100 times lower than for device B, making $1/\tau_{nr}$ the dominating term in Eq. (23) and giving the low 3dB-bandwidth compared to device B. Another way of expressing the behavior is that the Purcell enhancement only affects the carriers associated with transitions within the bandwidth of the cavity resonance. When the cavity resonance is much narrower than the electronic bandwidth the influence from the enhanced spontaneous emission only has a small effect on the total carrier density life time and thus also the speed.

#126340 - $15.00 USD Received 31 Mar 2010; revised 6 May 2010; accepted 9 May 2010; published 12 May 2010

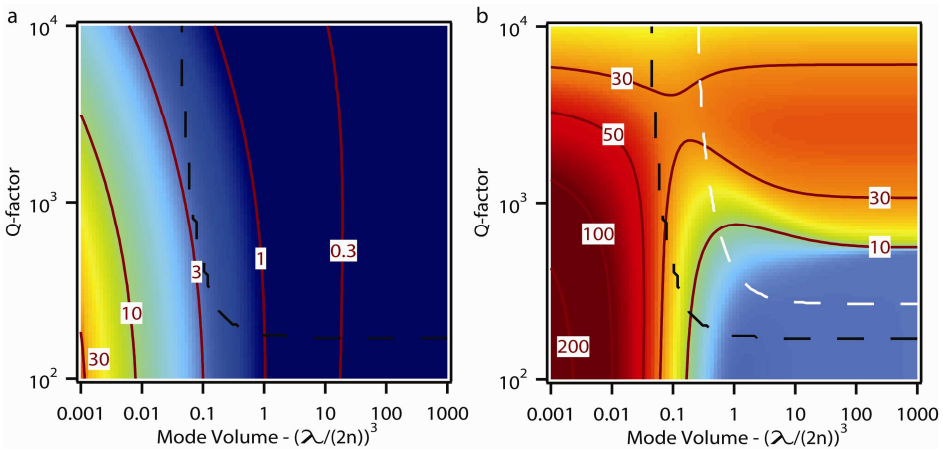

Fig. 4. The 3dB-bandwidth for a) $J = J_0$ and b) $J = 100\ J_0$. The red lines are contours of equal 3dB-bandwidth in GHz. The black line separates the potential laser devices from the LED devices and the white line indicates which of the laser devices that have larger stimulated emission than spontaneous emission at the given pump.

In order to examine the modulation bandwidth for a large range of devices, the 3dB-bandwidth has been calculated in the full model versus Q-factor and mode volume for a range of devices and the result is plotted in Fig. 4 for $J = J_0$ and $J = 100\ J_0$. The white line in the figure shows, for the given pump current, the device parameters for which stimulated and spontaneous emission are equal in magnitude. Devices to the right of this boundary are dominated by stimulated emission. The black line shows the limiting value of this boundary for large pump current, i.e. devices to the left of this line will always be dominated by spontaneous emission, independently of the strength of the pump, and are thus always in the LED regime.

All the devices in Fig. 4a are dominated by spontaneous emission for the given pump and are therefore in the LED regime. It is seen that the 3dB-bandwidth is below 3 GHz for most devices, except at extremely low mode volumes, which are probably unattainable in practice, where the bandwidth starts to increase. This is due to the effective Purcell factor, which is large at low mode volume, so that the first term in Eq. (23) dominates. The slight dependence on Q is due to the photon life time that becomes smaller at low Q and thereby increases the 3dB-bandwidth in Eq. (21).

The same dependence on Q is seen in Fig. 4b, where the 3dB-bandwidth exceeds 200 GHz in the lower left corner, i.e. in the LED regime. In the top right area, which corresponds to conventional laser structures, the effective Purcell factor saturates at a Q of a few hundreds and the stimulated emission therefore becomes the dominant recombination process so that the term aS_0/τ_p in Eq. (6) becomes large, giving the large modulation speed in this area. In the lower right corner the photon loss is too large to meet the lasing condition and the effective Purcell factor is low, giving the lower 3dB-bandwidth. In general the ultrahigh modulation speeds previously reported [6] are not seen, neither at low or high pump, because the effective Purcell factor saturates and becomes independent of the Q-factor as discussed above.

We note that for two level structures, such as quantum dot devices the upper left corner of Fig. 4a and b may correspond to devices operating in the strong coupling regime [11], where the calculated 3dB-bandwidth would be invalid. However, for quantum well structures and operation at room temperature, as considered here, this is not considered to be an issue.

Discussion and conclusions

In this paper we have discussed how to treat Purcell enhancement of spontaneous emission in quantum well nanoLEDs and nanolasers in the laser rate equation model. In the present model for the spontaneous emission rate, which incorporates details about the optical density-of-states, it was shown that the spontaneous emission rate saturates for high carrier density and

#126340 - $15.00 USD Received 31 Mar 2010; revised 6 May 2010; accepted 9 May 2010; published 12 May 2010

that it does not follow the usual linear enhancement with the cavity Q-factor. The independence of the Q-factor was found to originate from the cavity bandwidth being small compared to the electronic density-of-states and this limits the magnitude of the enhancement of the spontaneous emission in nanocavity systems. We introduced an effective Purcell enhancement that incorporates the important features due to the optical and electronic density-of-states and can be used to describe the spontaneous emission in a simple way. The limited effective Purcell enhancement entails that for devices with mode volumes attainable with today's technology the highest modulation bandwidth is found above threshold and limited by well-known damping effects due to gain nonlinearities [6,18]. The ultrafast modulation speeds previously reported in ref [6]. are only found in devices with extremely low mode volume and even for these devices the 3dB-bandwidth is below a few hundred GHz and the spectral bandwidth is very broad making wavelength division multiplexing systems difficult.

The limited modulation bandwidth is due to the wide electronic density-of-states as compared to the cavity spectrum. However, it can also be seen from Eq. (17) that if the electronic density-of-states function is narrower than the cavity bandwidth the saturation of the effective Purcell factor is lifted. This indicates that ultra-high bandwidths may be obtainable in quantum dot systems. However, it will be necessary to include inhomogeneous broadening in the analysis of quantum dot systems as this effect will widen the electronic density-of-states significantly. The same is true for the homogeneous broadening, which will be present even if the inhomogeneous broadening is made insignificant. A rigorous treatment of quantum dot systems is beyond the scope of this paper and whether the ultra-high modulation speeds are attainable in quantum dot systems remains an open question.

Acknowledgements

The authors would like to thank Michael Lorke for helpful discussions and Villum Fonden for financial support via the NATEC (Nanophotonics for TErabit Communications) center.

#126340 - $15.00 USD Received 31 Mar 2010; revised 6 May 2010; accepted 9 May 2010; published 12 May 2010